Powder Technology 424 (2023) 118520

Contents lists available at ScienceDirect

Powder Technology

journal homepage: www.journals.elsevier.com/powder-technology

Impact of material properties and process parameters on tablet quality in a continuous direct compression line

Pauline H.M. Janssen [a,b,*], Sara Fathollahi [b], Bram Bekaert [c], Dirk Vanderroost [d], Timo Roelofs [b], Valerie Vanhoorne [c], Chris Vervaet [c], Bastiaan H.J. Dickhoff [b]

[a] Department of Pharmaceutical Technology and Biopharmacy, University of Groningen, Antonius Deusinglaan 1, 9713, AV, Groningen, the Netherlands
[b] DFE Pharma, Klever Strasse 187, 47568 Goch, Germany
[c] Laboratory of Pharmaceutical Technology, Ghent University, Ottergemsesteenweg 460, 900 Gent, Belgium
[d] GEA Process engineering, Keerbaan 70, 2160 Wommelgem, Belgium

HIGHLIGHTS

- Blend properties of low-dose and high-dose formulations were evaluated with PLS
- Formulation behavior was mainly driven by the concentration of API
- Excipient properties also had a substantial impact on formulation behavior
- The relative performance of fillers differed for 1%*w*/w and 40% w/w formulations
- Processability of ingredients is crucial for formulation design

GRAPHICAL ABSTRACT

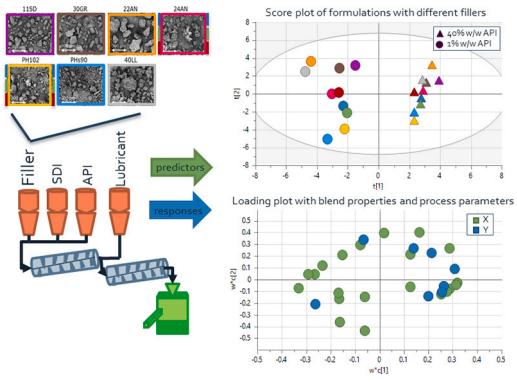

ARTICLE INFO

Keywords:
Continuous manufacturing
Continuous direct compression
Multivariate analysis
PLS regression
Tableting
Material characterization
Excipients
Lactose
Microcrystalline cellulose

ABSTRACT

The current paper shows how excipient properties impact the process parameters and the final tablet properties in a fully integrated continuous direct compression line. Blend properties of low-dose (1% *w*/w) and high-dose (40% w/w) paracetamol formulations were evaluated and linked to the blending and tableting performance via multivariate models (Partial Least Squares analysis, PLS). Feeding behavior was analyzed separately, as the amount of active pharmaceutical ingredient (API) that ended into tablets was driven by random fluctuations in the API feeding behavior. The developed PLS models elucidated that formulation behavior was mainly driven by the concentration of the active pharmaceutical ingredient (API), explained by the distinct API properties. Excipient properties also had a substantial impact on formulation behavior. Generally, formulations with microcrystalline cellulose as a filler showed better compactability, lower hold-up mass, lower flowability and higher cohesion than formulations with different lactose grades. The relative performance of a formulation with different fillers differed for 1% *w*/w and 40% w/w drug loading. Granular and spray dried lactose grades increased in compactability ranking compared to anhydrous lactose when evaluating higher drug loading, due to

* Corresponding author at: Department of Pharmaceutical Technology and Biopharmacy, University of Groningen, Antonius Deusinglaan 1, 9713, AV, Groningen, the Netherlands.
E-mail address: p.h.m.janssen@rug.nl (P.H.M. Janssen).

https://doi.org/10.1016/j.powtec.2023.118520
Received 7 March 2023; Received in revised form 31 March 2023; Accepted 3 April 2023
Available online 5 April 2023

the difference in morphology. It was shown that besides understanding the impact of excipients on the formulation performance, processability of ingredients is crucial for formulation design.

1. Introduction

The pharmaceutical industry is constantly searching for solutions that can improve manufacturing processes. Continuous operation is an approach that compared to batch-wise operation is considered to improve cost efficiency and product quality. Additionally, continuous operation provides improved efficiency and increased batch-size flexibility [1–4]. It is also encouraged by regulatory bodies, since it is in line with the Quality by Design paradigm for pharmaceutical development [5,6]. Continuous operation of production processes is getting a lot of attention in the industry, especially for the production of tablets by direct compression. In comparison to granulation techniques, direct compression has fewer manufacturing steps and pieces of equipment, reduced processing times, reduced labor costs, less process validation, lower consumption of powder, and there is no need to use heat or liquid in the process [7]. Unit operations of powder-to-tablet continuous direct compression (CDC) lines include feeding, blending and tableting. Other operating units, like milling or coating are optionally included.

In batch manufacturing processes for tablets, ingredients are typically dispensed in a blender and the product is removed from the process after each unit operation for offline quality testing. Continuous production processes in contrast generally consist of several unit operations that are combined through an automated control system [8,9]. At steady state conditions, the material is entering and exiting each unit operation at the same mass flow rate. Due to the inherent differences between batch and continuous processes, existing knowledge of batch manufacturing is not always directly transferable to continuous processes. Each individual processing step therefore has to be re-designed for continuous operation.

A continuous manufacturing process typically starts with feeding of raw material into the processing line [10]. The feeder performance determines the amount of a component that ends up in the final product and is therefore critical for product quality [11–13]. The inability to maintain targeted material concentrations in the process stream can lead to quality failures, such as out-of-specification dosage form assay and content uniformity [11,14,15]. Many authors have reviewed the importance of understanding the physical properties of raw materials and their impact on feeding [4,11,16–18]. Prior knowledge of physicochemical material properties can provide indications of how the powder will behave during processing and can support the optimal selection of feeder design. Material properties that are mentioned in the literature to be relevant for feeder performance include amongst others shape, particle size distribution, density, compressibility, and flow properties [11,16,19,20]. Due to the multi-variate nature of raw materials, however, it is typically not straightforward to determine which properties influence the feeding process most significantly [11,21]. Multivariate analysis (MVA) tools therefore have gained a lot of popularity for the evaluation of the impact of material properties on feeder performance [17,18,21–23]. The goal of the developed MVA models so far has been to predict the feeding behavior of new powders based on similarities in material properties. This allows optimal selection of the most suitable material, feeder capacity, feeding mechanism, and screw type, thereby leading to more efficient and faster development of new drug products.

The second step of a CDC line is blending, which typically is achieved by two consecutive continuous blenders. The first blender is used to blend materials that require intensive mixing, like the API and most of the excipients. The second blender is used to blend material from the first blender with additional materials that are shear-sensitive or require limited mixing, like lubricants. Blending is performed to create a formulation that allows manufacturing of constant unit doses by the tableting machine. The key criterium for mixing is to create a homogeneous blend, allowing consistent API delivery in each unit dose. Batch-wise powder blenders typically have a couple of limitations, including difficulty in scaling and flexibility [24]. Continuous blending processes do not have these issues, as the batch size is determined by the process run time rather than the blender size. Additionally, continuous blending typically results in better content uniformity than batch blending processes, provided that stable feeding is obtained for all components [13,25–27]. The homogeneity of a batch is shown to be more dependent on material properties of powders being mixed in a batch blending process than in a continuous blending process [13,25,27]. Research on continuous blending therefore primarily has been focused on the effect of process parameters and design [28–31].

The final step of a CDC line is the continuous tableting process. Commercial tableting processes are inherently continuous, and they can be combined with preceding unit operations to create a continuous process. In a batch-wise process, hoppers are typically filled in portions, while in a continuous process the hoppers are filled continuously. Due to its importance in batch-wise processing, the impact of material properties on compaction processes was intensively studied [32]. The success of the compaction process depends mainly on the material properties of the ingredients, especially their deformation behavior. Moisture content, surface properties, flow properties, particle size distribution, polymorphism, and amorphism are some of the properties that also have been identified to impact a compaction process [32–38]. Important to note is that even though specific material properties have been identified to impact a compaction process, efficient development of robust tableting processes is still experienced to be challenging due to the lack of mechanistic understanding of the impact of the complete set of raw material properties on tablet quality [39].

Many studies have been performed to understand the impact of material properties on individual unit operations, but limited research has been performed on fully integrated CDC lines. Research on fully integrated CDC lines has mainly been performed focusing on the effect of process parameters and process design [40–42], or on process analytical tools (PAT) and control strategies [43,44]. Additionally, case studies on challenging formulations have been performed. Formulation strategies for low-dose formulations [40], high-dose formulations [41,45] and formulations with a high segregation tendency [26,46] are reported. It was concluded that CDC lines are in particular useful for high drug load compositions of poorly flowing blends that could not be processed via batch manufacturing.

Limited studies have been performed so far to directly correlate the impact of material properties on the final product quality in a fully integrated CDC line. The relevance of evaluation in integrated systems is however often acknowledged, as the combination of the separate unit operations will determine the final product quality. For example the acceptable feeding variation depends on the downstream process and the performance of the blender to dampen out feeder fluctuations [20]. Studies investigating integrated CDC lines mainly have been focused on specific formulations and do not quantify correlations between the material properties and CDC responses [47]. In the current paper, the impact of excipient properties on the process parameters and the final tablet properties in a fully integrated CDC line was investigated. In this integrated study, blend properties of low-dose (1% *w*/w) and high-dose (40% w/w) formulations with ten different filler combinations are evaluated and linked via partial least squares (PLS) regression to the blending and tableting performance. It is the first time that a structured approach was used to evaluate both low and high dose formulations with such a variety of fillers.

2. Materials and methods

2.1. Materials

Spray dried lactose (SuperTab® 11SD), granulated lactose monohydrate (SuperTab® 30GR), anhydrous lactose (SuperTab® 22AN), granulated anhydrous lactose (SuperTab® 24AN), microcrystalline cellulose (Pharmacel® 102), silicified microcrystalline cellulose (Pharmacel® sMCC90) and co-processed lactose-lactitol (SuperTab® 40LL) were obtained from DFE Pharma (Goch, Germany). Twenty different formulations were produced with sodium starch glycolate (Primojel®, DFE Pharma, Goch, Germany), magnesium stearate (technical grade, Sigma Aldrich, Saint Louis, MO, USA) and paracetamol powder (Acetaminophen USP/Paracetamol Ph Eur Powder, Mallinckrodt, Raleigh, NC, USA) as indicated in Table 1.

2.2. Blend characterization

A blend of 2 kg for each formulation (F1 till F20) was produced using a tumbling mixer (Inversina Turbula 20 L, Bioengineering AG, Switzerland). All ingredients excluding the lubricant were transferred into a drum and blended at 25 rpm for 15 min at a fill volume of approximately 60% *v*/v. Magnesium stearate was added and blended for an additional 5 min at 15 rpm. Blends were characterized for particle size, compressibility, permeability, density and porosity, flow, and wall friction angle using the protocols described by Van Snick et al. [22].

All formulations were compressed using a STYL'One Evolution compaction simulator (Medelpharm, Beynost, France) with 10 mm cylindrical flat beveled Euro B punches (Natoli Engineering Company, Saint Charles, MO, USA). Tablets were compressed at six main compression forces (5, 10, 15, 20, 25 and 30 kN) with a fixed precompression force of 1.5 kN. A compression profile simulating the MODUL P rotary tablet press was used at a simulated turret speed of 50 rpm and an upper punch penetration depth of 3.25 mm. Target tablet weight and overfill level were set at 175.4 mg and 2 mm, respectively. Tablets were collected at the predefined compression forces and analyzed on tablet crushing force (SmartTest 50, Sotax, Basel, Switzerland). The compactability (Comp. at plateau) was defined as the plateau and/or peak value of the tensile strength. Tablets produced at the peak tensile strength were used to calculate the in-die yield strength (PyS) via linear regression of the linear portion of the Heckel plot [48,49], according to:

$$-ln\varepsilon = \frac{1}{PyS} \bullet P + A \quad (1)$$

The in-die porosity (ε) was calculated from the tablet thickness and diameter measured with the compaction simulator, while tablet weight and true density were determined after ejection.

Table 2 provides an overview of characterization methods, material descriptors and their abbreviations.

2.3. Continuous Direct Compression (CDC) evaluation

Continuous Direct Compression (CDC) trials of the twenty different formulations were performed on a ConsiGma® CDC 120LB2 - MS line (GEA, Wommelgem, Belgium), of which a schematic overview is provided in Fig. 1. Three different feeders containing paracetamol, superdisintegrant and a filler were integrated with the first continuous blender, and an additional feeder with lubricant was integrated with a second continuous blender. The final blend was compacted on an integrated tablet press (MODUL S, GEA, Wommelgem, Belgium).

2.3.1. Feeding set-up

Based on prior experimental determination, the feeders for the filler, paracetamol and superdisintegrant were geared with coarse concave screws (gear ratios of 63:1, 235:1 and 235:1 respectively). The feeder for

Table 1
Overview of the %w/w composition of twenty different formulations (F) that were evaluated. An additional column indicating the used abbreviations (abbr.) of the different fillers is included for clarification.

Excipient	abbr.	F1	F2	F3	F4	F5	F6	F7	F8	F9	F10	F11	F12	F13	F14	F15	F16	F17	F18	F19	F20
SuperTab® 11SD (% w/w)	11SD	94	55																		
SuperTab® 30GR (% w/w)	30GR			94	55																
SuperTab® 22AN (% w/w)	22AN					94	55														
SuperTab® 24AN (% w/w)	24AN							94	55			70.5	41.25	47	27.5	23.5	13.75				
Pharmacel® 102 (% *w*/w)	PH102									94	55	23.5	13.75	47	27.5	70.5	41.25				
Pharmacel® sMCC 90 (% *w*/w)	PHs90																	94	55		
SuperTab® 40LL (% w/w)	40LL																			94	55
Primojel® (% w/w)	PJ	4	4	4	4	4	4	4	4	4	4	4	4	4	4	4	4	4	4	4	4
Magnesium Stearate (% w/w)	MgSt	1	1	1	1	1	1	1	1	1	1	1	1	1	1	1	1	1	1	1	1
Paracetamol Powder (% *w*/w)	P_P	1	40	1	40	1	40	1	40	1	40	1	40	1	40	1	40	1	40	1	40

Table 2
Overview of the characterization methods, blend descriptors, and their respective abbreviations.

Characterization method	Descriptor	Abbreviation
Malvern	The size below which 10% v/v of the particles is found (μm)	x10
	The size below which 50% v/v of the particles is found [median size] (μm)	x50
	The size below which 90% v/v of the particles is found (μm)	x90
Flowpro	Flow through an orifice (mg/s)	FP
FT4 powder rheometer	Compressibility at 15 kPa (%)	C_15kPa
	Permeability at 15 kPa (mbar)	k_15kPa
Helium pycnometer	True density (g/mL)	ρtrue
	Bulk density (g/mL)	ρb
Tapping device	Tapped density (g/mL)	ρt
	Hausner ratio (−)	HR
Ring shear tester	Effective angle of internal friction (°)	φint
	Cohesion (Pa)	τc
	Flow function coefficient (−)	ffc
	Major principal stress (Pa)	MPS
	Unconfined yield stress (Pa)	UYS
	Wall friction angle (°)	WFA
Compaction Simulator	Compactability (MPa)	Comp. at plateau
	Yield strength (MPa)	PyS

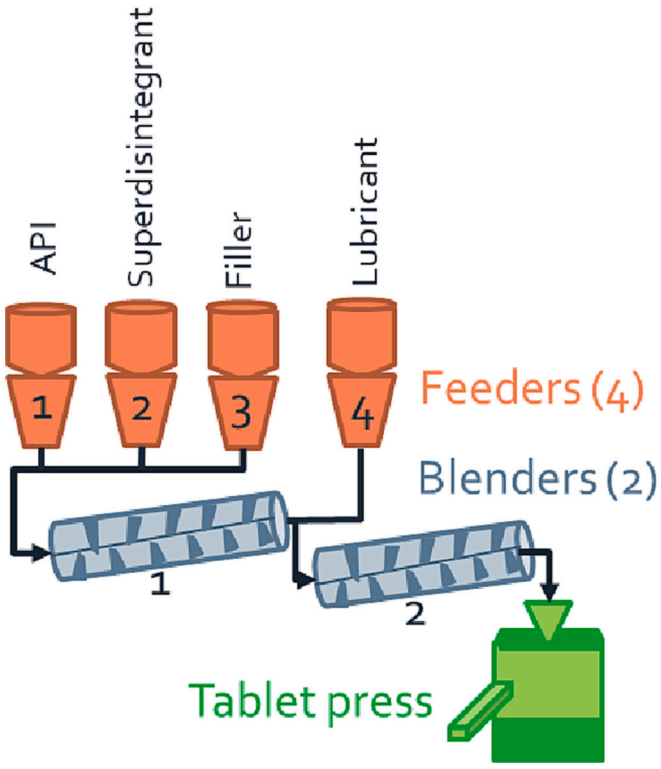

Fig. 1. Schematic overview of the ConsiGma® CDC 120LB2 - MS line. Three different feeders were integrated with the first continuous blender, and an additional feeder with lubricant was integrated with a second continuous blender. The final blend was compacted with an integrated tablet press.

magnesium stearate was geared with a fine concave screw (gear ratio 455:1) and an additional outlet mesh of 2 mm. *Re*-filling of the hoppers of the top-up systems for good flowing materials (i.e. fillers and superdisintegrant) was performed with pneumatic transport, while re-filling of the hoppers of the top-up systems for more cohesive components (i.e. paracetamol and magnesium stearate) was performed in a gravimetric mode with poly-ethylene bottles. When multiple fillers were used, one feeder was used for feeding a pre-blend of the fillers. Pre-blends were created by blending for 15 min at 25 rpm on a 60 L IBC blender with a fill volume of approximately 60% *v*/v. The speed of the feeder screws was optimized by the feeder control system to ensure a total system flow rate of 20 kg/h. Feeder data was collected every second, and feeding variability was determined on a 1 s timescale.

2.3.2. Blending set-up

The main blender was equipped with 11 centered radial mixing blades (RMB) rotating at 300 rpm for most trials. Formulations F1, F2, F7, F8, F9 and F10 were also tested with radial mixing blades rotating at 200 rpm, but were not considered for further analyses. The lubricant blender was equipped without radial mixing blades and rotates at 200 rpm. Fill levels in the blender were determined by stopping the blender instantaneously and collecting the powder mass pneumatically.

2.3.3. Tableting set-up

The MODUL S tablet press was equipped with 38 punches with 8 mm round flat beveled Euro B punches (Natoli Engineering Company, Saint Charles, MO, USA) with a score line in order to produce tablets with a target tablet weight of 175.4 mg. The turret speed was set to 50 rpm to match the system flow rate of 20 kg/h. Two standard curved paddles rotating at 58 rpm and 70 rpm were installed in the forced feeder. The pre-compression force was set to 1.5 kN and the target main compression force was 10 kN. During the process, no control loops were activated. After 5 min of running at the correct settings, sampling of tablets was initiated. Thirty consecutive grab samples of 20 s were collected. The target compression force was changed to 5 and 15 kN and after 5 min of steady state processing at each of these compression forces one sample of 20 s was collected.

2.4. Tablet analyses

Twenty randomly selected tablets from all uneven sample bags were analyzed on tablet crushing force, weight, diameter and thickness (n = 20) using an automated tablet tester (Sotax AT50, Basel, Switzerland). The force to break the tablet is measured at a constant speed of 2 mm/s, and the maximum force needed to break the tablet is used as tablet crushing force. The tablet tensile strength (TTS) is derived from the tablet crushing force (TCF), diameter (D) and tablet height (H) for flat beveled tablets [50]:

$$TTS = \frac{2 \bullet TCF}{\pi \bullet D \bullet H} \quad (2)$$

The porosity of the compacts is calculated from the tablet mass (m) and volume (V) and the true density (ρ_{true}) of the blend, according to:

$$\varepsilon_{tablet} = 1 - \frac{(m/V)}{\rho_{true}} \quad (3)$$

Three randomly selected tablets from sample bags 1, 5, 10, 15, 20, 25 and 30 of each formulation were evaluated with a UV-VIS spectrophotometer (Shimadzu UV-1650PC, Shimadzu Corporation, Kyoto, Japan) to determine the API concentration. Each tablet was dissolved and homogenized in 50 mL distilled water, diluted 1/50 times (for 1% *w*/w drug loading) or 1/200 times (for 40% w/w drug loading) and measured at a wavelength of 243 nm with a 1 cm cell.

2.5. Multi-variate analyses

SIMCA-P 16 (Umetric, Umeå, Sweden) was used to execute Partial Least Square (PLS) regression on the available data. The parameters in Table 2 and $\sigma_{MF,API}$, $\sigma_{MF,filler}$, $\sigma_{MF,PJ}$, $\sigma_{MF,MgSt}$, FD, PCH and MCH were considered as predictors (X), while the other parameters in Table 3 were included as response parameters (Y). Datasets were pre-treated prior to PLS regression via unit variance scaling and mean-centering. Next, log transformation was applied to non-normally distributed responses. Each

Table 3
Overview of the unit operations, collected responses, descriptors and corresponding abbreviation considered during multivariate analyses (MVA).

Unit operation	Descriptor	Abbreviation
Feeders	Mass flow variability [1 s] API (%)	$\sigma_{MF,API}$
	Mass flow variability [1 s] filler (%)	$\sigma_{MF,filler}$
	Mass flow variability [1 s] PJ (%)	$\sigma_{MF,PJ}$
	Mass flow variability [1 s] MgSt (%)	$\sigma_{MF,MgSt}$
	Feeder label claim (%)	FLC
	Feeder label claim variability [1 s] (%)	σ_{FLC}
Main and lubricant blender	Main blender hold-up mass (g)	HM_1
	Lubricant blender hold-up mass (g)	HM_2
Compression station	Fill depth (mm)	FD
	Pre-compression height (mm)	PCH
	Pre-compression displacement variability (%)	σPCD
	Main compression height (mm)	MCH
	Main compression height variability (%)	σCH
	Main compression force variability (%)	σCF
	Ejection force (N)	EF
Tablet analysis	Tablet tensile strength (MPa)	TS
	Tablet tensile strength variability (%)	σTS
	Tablet weight variability (%)	σMass
	Tablet porosity (−)	ε_t
Off-line UV-VIS spectrophotometry	Label claim (%)	LC
	Label claim variability (%)	σ_{LC}

model was optimized to increase the goodness of fit (R^2) and the predictive ability (Q^2). Variables with a poor fit (i.e. $R^2Y < 0.3$) or no significant correlation were removed from the models if their removal had a significant impact on the R^2 and Q^2 (i.e. R^2Y increased with >0.1). An additional principal component was included in the model when the component added new information, the R^2Y increased with >0.1, or when the Q^2 increased with >0.1. One model describing the twenty trials with 1% *w*/w and 40% *w*/w drug loading was created and optimized. Additionally, two separate models were developed for both the 1% w/w and 40% w/w drug loading trials to evaluate if the impact of fillers would differ for different API concentration.

3. Results and discussion

3.1. Processing challenges

The trials revealed some challenges that could happen during processing in an industrial environment. The processability of ingredients in a continuous direct compression line is therefore crucial in formulation design, on top of the expected properties of the final dosage form. Two types of observed challenges and potential ways to deal with them are outlined below.

The first type of challenges observed during trials was related to the compressibility and low fluidization potential of MCC (PH102). Ratholes were formed when this material was put under pressure, which required operator intervention. First of all, the pneumatic transport of this material was more challenging than for the other fillers, requiring manual vibration of the material packaging for the refill of the hopper. Additionally, the flow from the hopper into the feeders was often obstructed, requiring manual hammering of the hoppers. Hammering was also required during die filling of formulations from these fillers with both 1% and 40% *w*/w drug loading. During normal operation, the fill level of the feed tube for die filling is controlled via sensors, but dust formation of these formulations misled the sensors and required operator intervention. All these operator interventions increased the labor intensity, reduced the control and resulted in risks for obstructions in the process. Additionally, hammering could damage the equipment, providing a risk for abortion of the process.

The second type of challenges observed during execution of experiments was related to the rotational speed of the main blender. Six of the formulations were tested with 200 rpm as blending speed, of which two showed blending challenges. Formulations with 40% *w*/w drug loading and 11SD or 24AN as a filler resulted in material build-up in the blender and eventually blocking of the blender screw. It was hypothesized that the blender blockage in this case was related to the good flow properties of 24AN and 11SD, as flooding of these materials was observed in the blender and the header during these experiments. Flooding of these fillers through the conveying blades of the blender, combined with limited interaction of the filler with the paracetamol powder, could have resulted in accumulation of the paracetamol at the initial part of the blender [51]. Formulations with 40% *w*/w drug loading with PH102 as a filler did not show any issues in the blending. The cohesive nature of this powder blend resulted in the absence of flooding. Formulations with 1% *w*/w drug loading and PH102, 11SD or 24AN did also not show such issues in the blender, explained by the lower concentration of drug loading that results in lower risks for accumulation. Lastly, formulations that were blended with 300 rpm as rotational speed also showed no blending issues. Formulations blended with 300 rpm as rotation speed were therefore considered for further evaluation. Current observations therefore show the importance of alignment of process settings with material properties.

3.2. Feeder evaluation

No data obtained from the feeders ($\sigma_{MF,API}$, $\sigma_{MF,filler}$, $\sigma_{MF,PJ}$, $\sigma_{MF,MgSt}$, FLC, σ_{FLC}) and off-line UV-VIS spectrophotometry (LC, σ_{LC}) were included in the partial least squares (PLS) analyses, but data were evaluated separately. Data were excluded from the PLS as the R2Y for these parameters was below 0.3, indicating poor correlation with the other variables. The absence of a correlation between feeder data and the other variables was explained by the neglectable amount of variation in excipient feeding compared to the variation in API feeding, as can be observed in Table 4. API feeding was done before mixing with the excipient, and variation in the API content is therefore independent of the formulation composition.

Fillers showed a similar ranking on mass flow variability ($\sigma_{MF,Filler}$) when used for the 1% w/w and 40% w/w drug loading formulations (Supplementary Fig. 1). Mass flow variability of the fillers ($\sigma_{MF,Filler}$) varied from 0.3 to 4.5%, indicating that the properties of the filler have a substantial effect on the mass flow variability. Further research is recommended to correlate the filler properties to the mass flow variability in more detail. No correlation between the feeder label claim variability (σ_{FLC}) and the mass flow variability of the fillers ($\sigma_{MF,filler}$) was observed (Supplementary Fig. 2). In contrast, linear correlations between the feeder label claim variability (σ_{FLC}) and the mass flow variability of the API ($\sigma_{MF,API}$) with $R^2 > 0.9$ were observed for both 1% *w*/w drug loading and 40% w/w drug loading formulations (Supplementary Fig. 3). Fluctuations in the composition of the blend were therefore dominated by fluctuations in the API mass flow, which randomly varied over the different trials. The mass flow variability of the API was 8.2 ± 5.7% for 40% *w*/w drug loading formulations, while the mass flow variability of the API was 4.8 ± 2.4% for 1% w/w drug loading formulations. This was in contrast with previous research, as typically the API feeding consistency decreases at lower mass flow [15]. Higher mass flow variability for 40% *w*/w drug loading formulations was partly explained by bridging of the API in the feeder, which was more often observed at higher mass flow. Additionally, layering of the API on the screw surface was thought to have an impact. Screws were operated close to the upper limit of the screw speed for API feeding in the 40% *w*/w drug formulations, which provided limitations in potential adjustments when the feed factor of the screw (the amount of material delivered per revolution of the feeder

Table 4
Off-line UV-VIS spectrophotometry data (LC, σ_{LC}) and feeder response data (FLC, σ_{FLC}, $\sigma_{MF,API}$, $\sigma_{MF,filler}$, $\sigma_{MF,PJ}$, $\sigma_{MF,MgSt}$) of the twenty trials. No feeder data is available for F9, due to technical data acquisition issues during this trial.

Form.	API (%)	Filler	LC (%)	σ_{LC} (%)	FLC (%)	σ_{FLC} (%)	$\sigma_{MF,Filler}$ (%)	$\sigma_{MF,API}$ (%)	$\sigma_{MF,PJ}$ (%)	$\sigma_{MF,MgSt}$ (%)
F1	1	11SD	99.0	4.1	101.0	3.4	0.5	3.4	0.5	2.3
F2	40	11SD	99.7	1.8	98.4	14.6	1.3	14.5	2.3	4.3
F3	1	30GR	103.7	2.4	101.2	4.7	0.3	4.8	1.3	4.5
F4	40	30GR	103.1	3.5	99.1	1.9	0.3	3.1	2.9	2.1
F5	1	22AN	104.5	3.3	100.2	9.4	1.8	9.3	1.2	1.7
F6	40	22AN	100.7	1.5	99.4	2.6	2.5	3.6	2.8	3.5
F7	1	24AN	76.7	14.2	99.7	3.7	0.8	3.8	2.7	1.6
F8	40	24AN	99.1	2.9	99.8	1.6	0.8	2.5	2.4	2.7
F9	1	102	82.3	23.8	*not available due to technical issues					
F10	40	102	100.5	0.8	99.7	2.2	1.8	3.3	2.4	3.0
F11	1	24AN/PH102 (75:25)	100.2	1.6	102.9	6.5	4.3	4.4	1.8	2.1
F12	40	24AN/PH102 (75:25)	91.0	6.0	94.3	7.1	4.5	11.0	1.6	2.5
F13	1	24AN/PH102 (50:50)	81.5	15.7	96.3	8.5	1.1	8.6	2.7	1.7
F14	40	24AN/PH102 (50:50)	98.9	1.5	100.0	1.6	1.2	3.0	2.6	2.3
F15	1	24AN/PH102 (25:75)	103.0	2.7	99.4	2.9	1.6	2.6	2.1	2.1
F16	40	24AN/PH102 (25:75)	93.7	4.2	95.1	8.4	1.6	12.6	1.2	2.4
F17	1	PHs90	100.8	1.4	98.7	3.2	0.5	3.2	2.0	3.0
F18	40	PHs90	93.7	7.6	88.0	11.7	0.4	17.7	2.7	2.7
F19	1	40LL	103.1	2.0	100.7	3.3	0.8	3.2	2.0	2.0
F20	40	40LL	100.1	2.4	95.3	7.3	1.0	10.9	2.0	1.7

screw) reduced as the result of API layering on the screw surface. Layering of the API on the screw surface was confirmed by the higher variation in the feed factor and the increasing required screw speeds for 40% *w*/w drug loading formulations.

A correlation was observed between the off-line label claim values (LC) and the measured off-line label claim variability (σ_{LC}). When label claim (LC) values were substantially deviating from the target of 100%, higher label claim variability was observed. This correlation could be explained by coincidental inclusion of certain tablets from a timepoint with extremely deviating API concentrations. These tablets impacted both the label claim (LC) and the label claim variability (σ_{LC}) substantially.

No direct correlation between the feeder label claim variability (σ_{FLC}) and the measured off-line label claim variability (σ_{LC}) was observed. The absence of this correlation could be due to different factors. First of all, feeder label claim variability (σ_{FLC}) was calculated from the time period that gravimetric feeding was performed. During re-fill of the hoppers however, the feeders were running in volumetric mode. This time period could have a major effect on the actual label claim and label claim variability, although it was not included in the calculations [20]. In contrast, the off-line testing samples were collected at regular time intervals, which could coincide with a volumetric feeding period. Additionally, the number of samples and sample frequency used for determining the off-line label claim variability (σ_{LC}) can substantially impact the results. In this study, the label claim variability (σ_{LC}) was determined using 21 tablets, grouped in threes and sampled at seven different time points. The variability in API content observed in these 21 tablets may not accurately reflect the variability across a larger tablet population of approximately 19,000 tablets. Random sampling of tablets that deviate from the feeder label claim due to temporary feeder fluctuations had a significant impact on the off-line label claim variability (σ_{LC}). Selection of tablets that were not affected by these temporary fluctuations was impossible, due to the absence of PAT tools that could provide detailed real-time information or information on the residence time distribution of the material in the different operating units.

3.3. PLS model including both API concentrations

Fig. 2 shows the score and loading plot from the partial least squares (PLS) analyses of the available data for all twenty formulations. Besides the mentioned feeder and label claim data, hold-up mass in the lubricant blender (HM2), and the pre-compression displacement variability (σ_{PCD}) were removed from the model. R2Y values for these parameters were below 0.3, indicating poor correlation with the other variables. The hold-up mass in the lubricant blender (HM2) was not related to the formulation composition, as blender 2 was only used as a conveying line with fixed speed and configuration. The hold-up mass of this blender therefore only depended on the throughput of the processing lines, which was fixed to 20 kg/h. Pre-compression displacement variability (σ_{PCD}) was also not related to the formulation composition, because the pre-compression displacement was fixed at 0.2 mm and variability in this parameter is due to operational limitations. Coefficient plots for the different response parameters are provided in Supplementary Fig. 4 till Supplementary Fig. 7.

The score plot of the PLS model showed a clear horizontal split between formulations with a 1% *w*/w drug loading (left) and a 40% w/w drug loading (right). This horizontal grouping over principal component one (PC1) with an R2X of 0.46 suggests that the formulation behavior was mainly driven by the API concentration. Horizontal grouping by API concentration was explained by the distinct API properties that have a substantial impact on formulations with 40% *w*/w drug loading, while filler properties are less variable. The impact of the used filler was gradually observed over the vertical axis, with an R2X of 0.30. The vertical position of the used filler was similar for 1% *w*/w and 40% w/w drug loading formulations, and driven by the excipient properties. The vertical spread in the score plot was lower for 40% *w*/w formulations than for 1% w/w formulations, explained by the higher proportion of filler in 1% *w*/w formulations. No third component was included in the model, as the R2X of principle component 3 was only 0.06.

Parameters located at the left or right position in the loading plot represent parameters for which the variability was driven by the API concentration. Predictors that were substantially different for the used API compared to the fillers and for which the position is driven by the API concentration, include the true density (ρtrue), compactability parameters (PyS, Comp. at plateau), powder flow (FP, ffc) and cohesion indicators (τc, UYS, C_15kPa, HR, φint). True density was higher for formulations with 1% *w*/w drug loading, explaining the observed lower tablet porosity (ε_t) for these formulations. Compactability, tablet tensile strength (TS) and powder flow parameters were higher for formulations with 1% *w*/w drug loading, due to the higher amount of filler in these formulations. All used fillers are developed for use in direct compression processes and are therefore well compactable with easy to free flowing behavior and low cohesion. Cohesion is mainly driven by the API concentration and is higher for formulations with 40% *w*/w drug loading. Cohesion was also slightly higher for formulations containing microcrystalline cellulose (MCC) as a filler in the formulation, in line

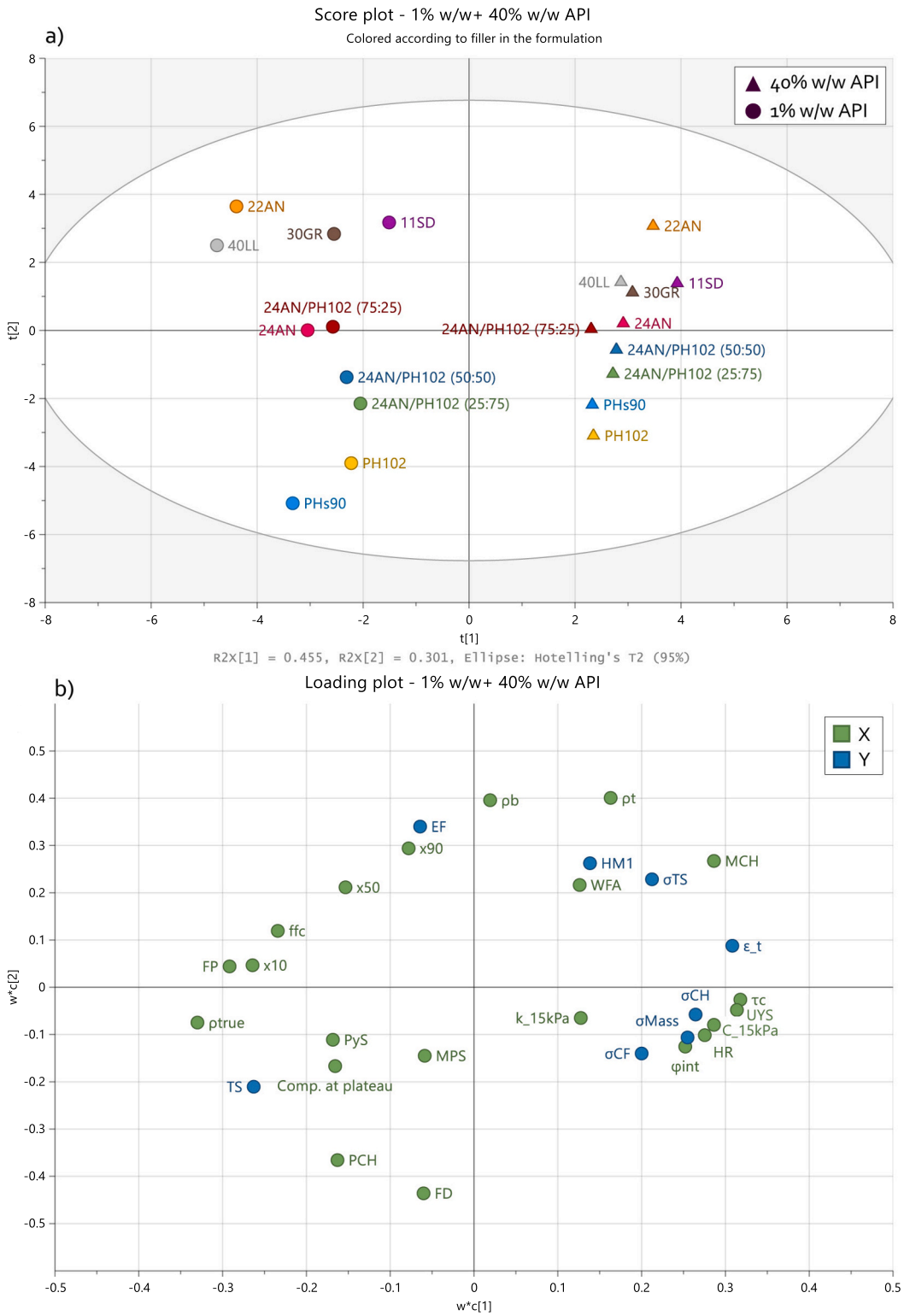

Fig. 2. Partial Least Squares score plot (a) and loading plot (b) for twenty formulations evaluated on a continuous direct compression line. Labels indicate the used filler(s) in the formulation, which were blended with 4% *w*/w superdisintegrant, 1% w/w magnesium stearate and 1% or 40% w/w paracetamol powder.

with high specific surface area of this material combined with the lower powder density [52], resulting in less gravitational forces that drive powder flow [53]. Higher cohesion results in higher fluctuations during die filling and consequently in variability of multiple tablet response parameters (σCH, σMass, σTS, σCF).

Formulations containing (silicified) MCC (PH102, PHs90) were located at the bottom of the score plot, followed by lactose/MCC blends with increasing lactose/MCC ratios (24AN/PH102 (25:75), 24AN/PH102 (50:50), 24AN/PH102 (75,25)), spray dried and granulated lactose grades (40LL, 30GR, 11SD) and anhydrous lactose (22AN). Parameters located at the top or bottom position in the loading plot represent parameters for which the variability was driven by the excipient type. The used API in this study had a median particle size of 32 μm, while the used fillers all have median particle sizes of 80 μm or

higher [52]. The fine part of the particle size distribution of the formulations was therefore highly impacted by the API concentration, while the coarser part was driven by the particle size of the filler. Additional predictors that drive the vertical spread of the formulations and were therefore driven by the properties of the used fillers included compactability related parameters (PyS, Comp. at plateau, MCH) and density related parameters (ρb, ρt, FD, PCH).

Compactability parameters were highest for plastically deforming MCC grades, in line with the higher tensile strength (TS) for this material. The variability in tensile strength (σTS) was inversely correlated to the tensile strength and therefore slightly higher for lactose formulations. Similar absolute variation in tensile strength results in lower relative variability when the tensile strength is higher. The main compression height (MCH) was also inversely correlated to compactability predictors of a material, explained by the force development during tableting which is higher when the compactability of a material is low. The ejection force (EF) was completely driven by the type of filler in the formulation, due to the high impact of deformation mechanism on this parameter. Brittle materials, located at the top of the score plot, create higher frictional forces with the die walls than plastic deforming materials. This relates to the presence of unlubricated surface at the tablet-die wall interface upon fracture during compaction [54]. Ejection force was also correlated to the main compression height during tableting. Higher main compression height results in higher tablet thickness. If more particle surface is available for contact with the die wall, larger ejection forces may be required to remove the compact.

Density related parameters were mainly driven by the type of filler used in the formulation, although for some parameters an impact of the API concentration was observed. Bulk density (ρb) and filling depth (FD) were mainly driven by the filler properties, as variability in bulk density of fillers spanned from 0.33 to 0.68 g/mL [52], while the API had a bulk density of 0.32 g/mL. Tapped density (ρt) was also impacted by the API concentration, as better packing efficiency could be obtained with a higher fines content as the result of higher drug loading [55]. Density parameters were located in the top part of the loading plot, indicating higher density for lactose formulations, with 22AN formulations having the highest density. The coefficient plots in Supplementary Fig. 4 indicated that the hold-up mass in blender 1 (HM1) was mainly driven by the bulk and tapped density of the formulations, related to the fixed volume that fits into the blender. The hold-up mass in blender 1 (HM1) varied from 1.0 to 2.2 kg. Larger hold-up mass might be beneficial when more mixing is required to achieve a good label claim variability. This can be especially relevant with unpredictable feeding performance of the API, as indicated in section 3.2 of this paper. In case the feeding performance of the filler is driving the label claim variability, larger hold-up masses might be required for formulations containing 24AN/PH102 (75:25), 22AN or PH102 as these fillers showed the highest mass flow variabilities of 1.8–4.5%. All other fillers showed mass flow variabilities below 1.6% and provide low risk for higher label claim variability. MCC grades did show the lowest hold-up mass and therefore the lowest amount of material that is in-process and at risk. Pre-compression height (PCH) was driven by differences in bulk density as well, as the initial force build-up during tableting originates from resistance of the powder for volume reduction.

A detailed explanation on the position of and the relationship between the different variables and response parameters is provided in Supplementary section A.

3.4. PLS models per API concentration

Fig. 3 shows the score and loading plots from the partial least squares (PLS) analyses of the available data for formulations with 1% *w*/w and 40% w/w drug loading. The ranking of excipients along the horizontal axis (PC1) was similar to the vertical ranking of excipients in the overall

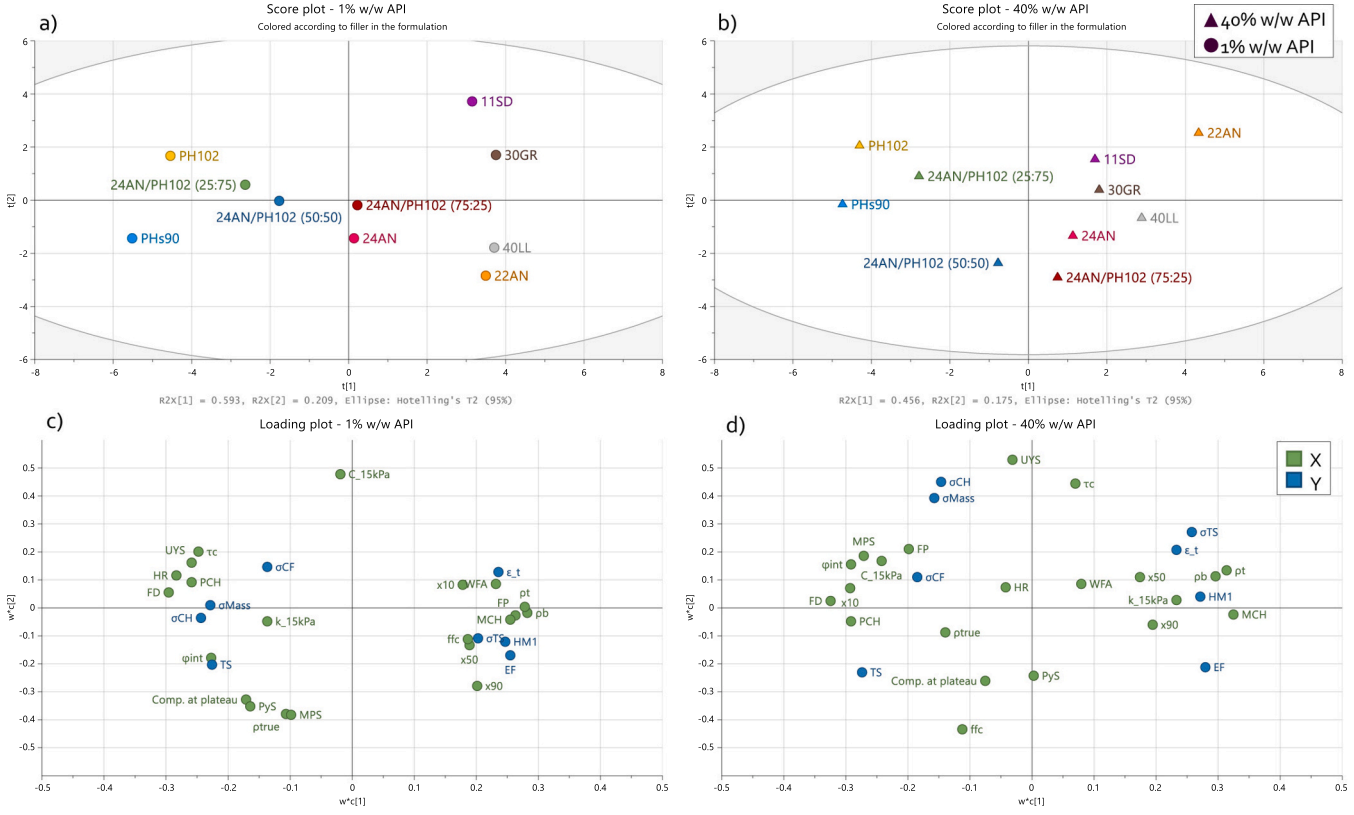

Fig. 3. Partial Least Squares score plots (a,c) and loading plots (b,d) for formulations with 1% *w*/w (a,c) and 40% *w*/w (b,d) drug loading, evaluated on a CDC line. Labels indicate the used filler(s) in the formulation, which were blended with 4% *w*/w superdisintegrant, 1% *w*/w magnesium stearate and 1% or 40% *w*/w paracetamol powder.

model (PC2), both representing the main drivers for formulation differences based upon excipient properties. The 1% *w*/w drug loading model had an R2X of 0.80, compared to an R2X of 0.63 for the 40% *w*/w drug loading model. The higher R2X of the 1% *w*/w was in line with the position of the formulations in the overall model, as a larger spread in the score plot for 1% *w*/w formulations was observed than for 40% *w*/w formulations.

Many correlations between parameters along PC2 in the overall model were observed along PC1 in the separate drug loading models, especially in the 1% *w*/w drug loading model. For example, compactability (PyS, Comp. at plateau) and powder flow (ffc, FP) were negatively correlated along PC2 in the overall model and negatively correlated along PC1 in the 1% *w*/w drug loading model. Similarly, cohesion (τc, UYS, C_15kPa, HR, φint) and compactability were positively correlated along PC2 in the overall model and positively correlated along PC1 in the 1% *w*/w drug loading model.

Focusing on one drug loading in a model however also revealed differences in correlations, depending on the API concentration. The PLS model with formulations containing 1% *w*/w API was driven from bottom-left to top-right by compaction parameters (PyS, Comp. at plateau), while from left/top-left to bottom-right/right it was driven by flow and cohesion parameters. Flow parameters (ffc, FP) were located on the right side of the loading plot, cohesion parameters (τc, UYS, HR, φint) were mainly located left/top-left, with tableting variability parameters (σCH, σMass, σCF) located in a similar direction. Tensile strength variability (σTS) was the exception, as this parameter was located on the right and inversely correlated to the tensile strength (TS) which was located towards the bottom-left. The compressibility at 15 kPa (C_15kPa) was the key driver along the PC2 axis, which was the main differentiator between the different lactose grades (11SD, 30GR, 40LL, 22AN). In general, 1% *w*/w drug loading formulations showed the highest tensile strength with the lowest hold-up mass and lowest ejection force for formulations containing MCC grades. In contrast, the lowest variability in tableting parameters (σCH, σMass, σCF) for 1% *w*/w formulations was observed for formulations with 22AN or 40LL.

The PLS model with formulations containing 40% *w*/w API was driven from bottom-left to top-right by compaction parameters, while from top-left till bottom-right mainly flow and cohesion parameters were driving the variability. Compared to the 1% *w*/w drug loading model, correlations between the parameters were different. Less grouping of flow (ffc, FP) and cohesion (τc, UYS, HR, φint) parameters was observed for the 40% *w*/w drug loading model, explained by the multidimensional character of flow [56], combined with the lower differentiation when evaluating formulations with higher drug loading. For example parameters unconfined yield strength (UYS), cohesion (τc) and flow function coefficient (ffc) were mainly located along PC1 in the 1% *w*/w drug loading model, while in the 40% *w*/w drug loading model they are located along the PC2 and are therefore less correlated to the other flow/cohesion (FP, HR, φint) parameters. In both models, flow through an orifice (FP) and the size below which 10% v/v of the particles is found (x10) were located along PC1 in the inverse direction of the permeability at 15 kPa (k_15kPa). For the 40% drug loading model however, flow through an orifice (FP) and the size below which 10% *v*/v of the particles is found (x10) are pointing towards the left, while for the 40% drug loading model these parameters point towards the right. Compressibility at 15 kPa (C_15kPa) was the main driver for PC2 in the 1% drug loading model, but is located along PC1 in the 40% drug loading model. Tableting variability parameters (σCH, σMass, σCF) were located in the top-left quadrant in the 40% drug loading model, having a high correlation with the effective angle of internal friction (φint) and the compressibility (C_15kPa). Tensile strength variability (σTS) was the exception, as this parameter was inversely correlated to the tensile strength (TS). In general, lowest variability in tableting parameters (σCH, σMass, σCF) combined with the highest hold-up mass and highest ejection force for 40% *w*/w formulations was observed for formulations containing 22AN or 40LL, followed by formulations with 24AN or 24AN/PH102 (75:25).

Both models showed a similar direction for compactability related parameters (Comp. at plateau, PyS, MCH, TS, σTS, EF) with highest compactability bottom-left and lowest compactability top-right. Ranking of filler-types in this direction was similar in both models, with MCC grades located in the bottom-left of the score plot, followed by blends with MCC, granular and spray dried lactose and anhydrous lactose in the top right. 22AN was the only filler that moved substantially in the ranking of materials. 22AN showed higher compactability than 11SD/30GR/40LL for formulations with 1% *w*/w drug loading, while for 40% *w*/w drug loading 22AN showed the lowest compactability. This change in position might be related to the morphology of the different lactose grades, as visualized in Fig. 4. Granular and spray dried lactose grades 11SD/30GR/40LL have more raspberry shaped morphologies with higher buffering capacity for the API. 22AN in contrast consists of larger shard shaped particles, explaining the lower relative ranking on compactability parameters with 40% *w*/w drug loading.

4. Conclusions

In the current paper, the impact of raw material properties on the process parameters and the final tablet properties in a fully integrated continuous direct compression (CDC) line was investigated. In this integrated study, blend properties of low-dose (1% *w*/w) and high-dose (40% *w*/w) formulations were evaluated and linked to the blending and tableting performance via multivariate models (Partial Least Squares analysis, PLS).

During the performed trials, a couple of challenges related to industrial processing were observed. Operator intervention was required when working with microcrystalline cellulose (MCC) with low fluidization potential. Additionally, formulations with 40% *w*/w drug loading could not be processed with good flowing fillers 11SD and 24AN at blending speeds of 200 rpm. These findings highlighted that the processability of materials in a CDC line is crucial in formulation design.

In this study, feeder label claim (FLC) and feeder content uniformity (σ_{FLC}) were driven by random fluctuations in the active pharmaceutical ingredient (API) feeding behavior. Higher mass flow variability for feeding 40% *w*/w drug loading was observed than for feeding 1% *w*/w drug loading, explained by bridging of the API in the feeder and layering of the API on the screw surface. No direct correlation between the feeder label claim variability (σ_{FLC}) and the measured off-line label claim variability (σ_{LC}) was observed. The absence of this correlation could be due to different factors, including volumetric feeding periods, and the number of samples and frequency of sampling for off-line testing.

The developed PLS models elucidated that formulation behavior was mainly driven by the API concentration, explained by the distinct API properties. Flow and compactability were positively correlated, as they were both lower for formulations with a high drug loading. Excipient properties also had a substantial impact on formulation behavior, with stronger impact in 1% *w*/w drug loading formulations than in 40% *w*/w drug loading formulations. Formulations with MCC showed better compactability, with lower flowability and higher cohesion than formulations with lactose.

The position of predictors and responses, and the ranking of the used filler in the formulation was different when looking at formulations with 1% *w*/w and 40% w/w drug loading. The change in position of the fillers might be related to the morphology of the different lactose grades, resulting in different loading capacity. In general, 1% *w*/w formulations provided highest tensile strength when MCC grades were used in the formulation, while the lowest variability in tableting parameters (σCH, σMass, σCF) could be achieved when using 22AN or 40LL. 40% *w*/w formulations provided the lowest variability in tableting parameters (σCH, σMass, σCF) combined with the highest hold-up mass and highest ejection force for formulations containing 22AN or 40LL, followed by formulations with 24AN or 24AN/PH102 (75:25).

In summary, this study showed how material properties and process

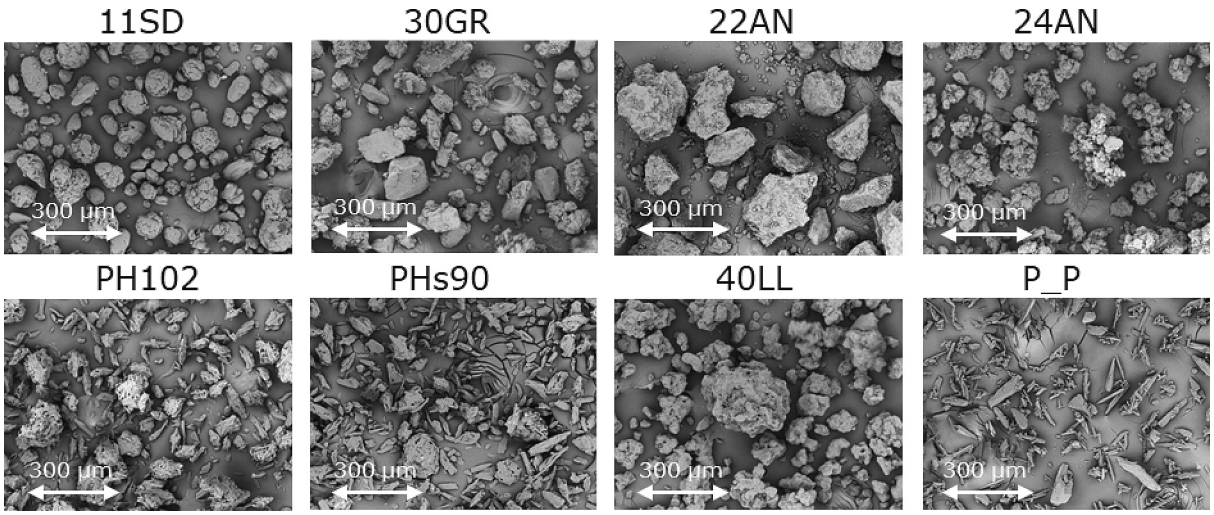

Fig. 4. Scanning Electron Microscopy (SEM) pictures of the different lactose grades, different microcrystalline cellulose grades and paracetamol grade used in this study.

parameters can play a crucial role in the optimization of CDC processes. Findings of this study can contribute to the speed and quality of formulation development.

Declaration of Competing Interest

None.

Data availability

Data will be made available on request.

Acknowledgement

The authors would like to thank Lisa Buijvoets for the support with execution of the trials.

Appendix A. Supplementary data

Supplementary data to this article can be found online at https://doi.org/10.1016/j.powtec.2023.118520.

References

[1] C.L. Burcham, A.J. Florence, M.D. Johnson, Continuous manufacturing in pharmaceutical process development and manufacturing, Annu. Rev. Chem. Biomol. Eng. 9 (2018) 253–281, https://doi.org/10.1146/annurev-chembioeng-060817-084355.
[2] M. Teżyk, B. Milanowski, A. Ernst, J. Lulek, Recent progress in continuous and semi-continuous processing of solid oral dosage forms: a review, Drug Dev. Ind. Pharm. 42 (2015) 1195–1214, https://doi.org/10.3109/03639045.2015.1122607.
[3] S.D. Schaber, D. Gerogiorgis, R. Ramachandran, J.M.B. Evans, P.I. Barton, B. L. Trout, Economic analysis of integrated continuous and batch pharmaceutical manufacturing: a case study, Ind. Eng. Chem. Res. 50 (2011) 10083–10092.
[4] F. Tahir, J. Palmer, J. Khoo, J. Holman, I.K. Yadav, G. Reynolds, E. Meehan, A. Mitchell, G. Bajwa, Development of feed factor prediction models for loss-in-weight powder feeders, Powder Technol. 364 (2020) 1025–1038, https://doi.org/10.1016/j.powtec.2019.09.071.
[5] S. Chatterjee, FDA perspective on continuous manufacturing, IFPAC Annu. Meet. Balt. MD 26 (2012) 34–42.
[6] S.L. Lee, T.F. O'Connor, X. Yang, C.N. Cruz, S. Chatterjee, R.D. Madurawe, C.M. V. Moore, L.X. Yu, J. Woodcock, Modernizing pharmaceutical manufacturing: from batch to continuous production, J. Pharm. Innov. 10 (2015) 191–199, https://doi.org/10.1007/s12247-015-9215-8.
[7] R.F. Shangraw, Compressed Tablets by Direct Compression Granulation Pharmaceutical Dosage Forms 1, 1989 (ISBN 0824780442.).
[8] M. Fonteyne, J. Vercruysse, F. De Leersnyder, B. Van Snick, C. Vervaet, J.P. Remon, T. De Beer, Process analytical Technology for Continuous Manufacturing of solid-dosage forms, TrAC - Trends Anal. Chem. 67 (2015) 159–166, https://doi.org/10.1016/j.trac.2015.01.011.
[9] J.M. Vargas, S. Nielsen, V. Cárdenas, A. Gonzalez, E.Y. Aymat, E. Almodovar, G. Classe, Y. Colón, E. Sanchez, R.J. Romañach, Process analytical Technology in Continuous Manufacturing of a commercial pharmaceutical product, Int. J. Pharm. 538 (2018) 167–178, https://doi.org/10.1016/j.ijpharm.2018.01.003.
[10] S.P. Simonaho, J. Ketolainen, T. Ervasti, M. Toiviainen, O. Korhonen, Continuous manufacturing of tablets with PROMIS-line - introduction and case studies from continuous feeding, blending and tableting, Eur. J. Pharm. Sci. 90 (2016) 38–46, https://doi.org/10.1016/j.ejps.2016.02.006.
[11] C.A. Blackshields, A.M. Crean, Continuous powder feeding for pharmaceutical solid dosage form manufacture: a short review, Pharm. Dev. Technol. 23 (2018) 554–560, https://doi.org/10.1080/10837450.2017.1339197.
[12] J. Hanson, Control of a system of loss-in-weight feeders for drug product continuous manufacturing, Powder Technol. 331 (2018) 236–243, https://doi.org/10.1016/j.powtec.2018.03.027.
[13] M. Jaspers, M.T.W. de Wit, S.S. Kulkarni, B. Meir, P.H.M. Janssen, M.M.W. van Haandel, B.H.J. Dickhoff, Impact of excipients on batch and continuous powder blending, Powder Technol. 384 (2021) 195–199, https://doi.org/10.1016/j.powtec.2021.02.014.
[14] L. Pernenkil, C.L. Cooney, A review on the continuous blending of powders, Chem. Eng. Sci. 61 (2006) 720–742, https://doi.org/10.1016/j.ces.2005.06.016.
[15] S. Sacher, N. Heindl, J.A. Afonso Urich, J. Kruisz, J.G. Khinast, A solution for low-dose feeding in continuous pharmaceutical processes, Int. J. Pharm. 591 (2020), 119969, https://doi.org/10.1016/j.ijpharm.2020.119969.
[16] W.E. Engisch, F.J. Muzzio, Loss-in-weight feeding trials case study: pharmaceutical formulation, J. Pharm. Innov. 10 (2015) 56–75, https://doi.org/10.1007/s12247-014-9206-1.
[17] N. Bostijn, J. Dhondt, A. Ryckaert, E. Szabó, W. Dhondt, B. Van Snick, V. Vanhoorne, C. Vervaet, T. De Beer, A multivariate approach to predict the volumetric and gravimetric feeding behavior of a low feed rate feeder based on raw material properties, Int. J. Pharm. 557 (2019) 342–353, https://doi.org/10.1016/j.ijpharm.2018.12.066.
[18] M.S. Escotet-Espinoza, S. Moghtadernejad, J. Scicolone, Y. Wang, G. Pereira, E. Schäfer, T. Vigh, D. Klingeleers, M. Ierapetritou, F.J. Muzzio, Using a material property library to find surrogate materials for pharmaceutical process development, Powder Technol. 339 (2018) 659–676, https://doi.org/10.1016/j.powtec.2018.08.042.
[19] W.K. Hsiao, T.R. Hörmann, P. Toson, A. Paudel, P. Ghiotti, F. Stauffer, F. Bauer, S. Lakio, O. Behrend, R. Maurer, et al., Feeding of particle-based materials in continuous solid dosage manufacturing: a material science perspective, Drug Discov. Today 25 (2020) 800–806, https://doi.org/10.1016/j.drudis.2020.01.013.
[20] W.E. Engisch, F.J. Muzzio, Feedrate deviations caused by hopper refill of loss-in-weight feeders, Powder Technol. 283 (2015) 389–400, https://doi.org/10.1016/j.powtec.2015.06.001.
[21] Y. Wang, T. Li, F.J. Muzzio, B.J. Glasser, Predicting feeder performance based on material flow properties, Powder Technol. 308 (2017) 135–148, https://doi.org/10.1016/j.powtec.2016.12.010.
[22] B. Van Snick, J. Dhondt, K. Pandelaere, J. Bertels, R. Mertens, D. Klingeleers, G. Di Pretoro, J.P. Remon, C. Vervaet, T. De Beer, et al., A multivariate raw material property database to facilitate drug product development and enable in-silico design of pharmaceutical dry powder processes, Int. J. Pharm. 549 (2018) 415–435, https://doi.org/10.1016/j.ijpharm.2018.08.014.
[23] B. Bekaert, L. Penne, W. Grymonpré, B. Van Snick, J. Dhondt, J. Boeckx, J. Vogeleer, T. De Beer, C. Vervaet, V. Vanhoorne, Determination of a quantitative relationship between material properties, process settings and screw feeding behavior via multivariate data-analysis, Int. J. Pharm. 602 (2021), https://doi.org/10.1016/j.ijpharm.2021.120603.

[24] W.J. Roth, A. Almaya, T.T. Kramer, J.D. Hofer, A demonstration of mixing robustness in a direct compression continuous manufacturing process, J. Pharm. Sci. 106 (2017) 1339–1346, https://doi.org/10.1016/j.xphs.2017.01.021.
[25] M. Jaspers, S.S. Kulkarni, F. Tegel, T.P. Roelofs, M.T.W. de Wit, P.H.M. Janssen, B. Meir, R. Weinekötter, B.H.J. Dickhoff, Batch versus continuous blending of binary and ternary pharmaceutical powder mixtures, Int. J. Pharm. X 4 (2022), https://doi.org/10.1016/j.ijpx.2021.100111.
[26] A.P. Karttunen, H. Wikström, P. Tajarobi, M. Fransson, A. Sparén, M. Marucci, J. Ketolainen, S. Folestad, O. Korhonen, S. Abrahmsén-Alami, Comparison between integrated continuous direct compression line and batch processing – the effect of raw material properties, Eur. J. Pharm. Sci. 133 (2019) 40–53, https://doi.org/10.1016/j.ejps.2019.03.001.
[27] S. Oka, A. Sahay, W. Meng, F. Muzzio, Diminished segregation in continuous powder mixing, Powder Technol. 309 (2017) 79–88, https://doi.org/10.1016/j.powtec.2016.11.038.
[28] J. Palmer, G.K. Reynolds, F. Tahir, I.K. Yadav, E. Meehan, J. Holman, G. Bajwa, Mapping key process parameters to the performance of a continuous dry powder blender in a continuous direct compression system, Powder Technol. 362 (2020) 659–670, https://doi.org/10.1016/j.powtec.2019.12.028.
[29] A.U. Vanarase, F.J. Muzzio, Effect of operating conditions and design parameters in a continuous powder mixer, Powder Technol. 208 (2011) 26–36, https://doi.org/10.1016/j.powtec.2010.11.038.
[30] Y. Gao, A. Vanarase, F. Muzzio, M. Ierapetritou, Characterizing continuous powder mixing using residence time distribution, Chem. Eng. Sci. 66 (2011) 417–425, https://doi.org/10.1016/j.ces.2010.10.045.
[31] M.A. Järvinen, J. Paaso, M. Paavola, K. Leiviskä, M. Juuti, F. Muzzio, K. Järvinen, Continuous direct tablet compression: effects of impeller rotation rate, Total feed rate and drug content on the tablet properties and drug release, Drug Dev. Ind. Pharm. 39 (2013) 1802–1808, https://doi.org/10.3109/03639045.2012.738681.
[32] S. Patel, A.M. Kaushal, A.K. Bansal, Compression physics in the formulation development of tablets, Crit. Rev. Ther. Drug Carrier Syst. 23 (2006) 1–65, https://doi.org/10.1615/critrevtherdrugcarriersyst.v23.i1.10.
[33] S. Jain, Mechanical Properties of Powders for Compaction and Tableting : An Overview, **1999**, p. *2*.
[34] C.C. Sun, A classification system for tableting behaviors of binary powder mixtures, Asian J. Pharm. Sci. 11 (2016) 486–491, https://doi.org/10.1016/j.ajps.2015.11.122.
[35] M. Šimek, V. Grünwaldová, B. Kratochvíl, Comparison of Compression and Material Properties of Differently Shaped and Sized Paracetamols †. 34, 2017, pp. 197–206, https://doi.org/10.14356/kona.2017003.
[36] M. Jivraj, L.G. Martini, C.M. Thomson, C.M. Thomson, An Overview of the Different Excipients Useful for the Direct Compression of Tablets, **2000**, p. *3*.
[37] N. Tarlier, I. Soulairol, B. Bataille, G. Baylac, P. Ravel, I. Nofrerias, P. Lefèvre, T. Sharkawi, Compaction behavior and deformation mechanism of directly compressible textured mannitol in a rotary tablet press simulator, Int. J. Pharm. 495 (2015) 410–419, https://doi.org/10.1016/j.ijpharm.2015.09.007.
[38] A. Mehrotra, B. Chaudhuri, A. Faqih, M.S. Tomassone, F.J. Muzzio, A modeling approach for understanding effects of powder flow properties on tablet weight variability, Powder Technol. 188 (2009) 295–300, https://doi.org/10.1016/j.powtec.2008.05.016.
[39] J. Dhondt, J. Bertels, A. Kumar, D. Van Hauwermeiren, A. Ryckaert, B. Van Snick, D. Klingeleers, C. Vervaet, T. De Beer, A multivariate formulation and process development platform for direct compression, Int. J. Pharm. 623 (2022), 121962, https://doi.org/10.1016/j.ijpharm.2022.121962.
[40] B. Van Snick, J. Holman, V. Vanhoorne, A. Kumar, T. De Beer, J.P. Remon, C. Vervaet, Development of a continuous direct compression platform for low-dose drug products, Int. J. Pharm. 529 (2017) 329–346, https://doi.org/10.1016/j.ijpharm.2017.07.003.
[41] B. Van Snick, J. Holman, C. Cunningham, A. Kumar, J. Vercruysse, T. De Beer, J. P. Remon, C. Vervaet, Continuous direct compression as manufacturing platform for sustained release tablets, Int. J. Pharm. 519 (2017) 390–407, https://doi.org/10.1016/j.ijpharm.2017.01.010.
[42] S.C. Galbraith, S. Park, Z. Huang, H. Liu, R.F. Meyer, M. Metzger, M.H. Flamm, S. Hurley, S. Yoon, Linking process variables to residence time distribution in a hybrid flowsheet model for continuous direct compression, Chem. Eng. Res. Des. 153 (2020) 85–95, https://doi.org/10.1016/j.cherd.2019.10.026.
[43] Y. Suzuki, H. Sugiyama, M. Kano, R. Shimono, G. Shimada, R. Furukawa, E. Mano, K. Motoyama, T. Koide, Y. Matsui, et al., Control strategy and methods for continuous direct compression processes, Asian J. Pharm. Sci. 16 (2021) 253–262, https://doi.org/10.1016/j.ajps.2020.11.005.
[44] K. Järvinen, W. Hoehe, M. Järvinen, S. Poutiainen, M. Juuti, S. Borchert, In-line monitoring of the drug content of powder mixtures and tablets by near-infrared spectroscopy during the continuous direct compression tableting process, Eur. J. Pharm. Sci. 48 (2013) 680–688, https://doi.org/10.1016/j.ejps.2012.12.032.
[45] T. Ervasti, H. Niinikoski, E. Mäki-Lohiluoma, H. Leppinen, J. Ketolainen, O. Korhonen, S. Lakio, The comparison of two challenging low dose APIs in a continuous direct compression process, Pharmaceutics 12 (2020) 1–19, https://doi.org/10.3390/pharmaceutics12030279.
[46] S. Lakio, T. Ervasti, P. Tajarobi, H. Wikström, M. Fransson, A.P. Karttunen, J. Ketolainen, S. Folestad, S. Abrahmsén-Alami, O. Korhonen, Provoking an end-to-end continuous direct compression line with raw materials prone to segregation, Eur. J. Pharm. Sci. 109 (2017) 514–524, https://doi.org/10.1016/j.ejps.2017.09.018.
[47] B. Bekaert, B. Van Snick, K. Pandelaere, J. Dhondt, G. Di Pretoro, T. De Beer, C. Vervaet, V. Vanhoorne, Continuous direct compression: development of an empirical predictive model and challenges regarding PAT implementation, Int. J. Pharm. X 4 (2022), 100110, https://doi.org/10.1016/j.ijpx.2021.100110.
[48] R.W. Heckel, Density-pressure relationship in powder compaction, Trans. Met. Soc., AIME 221 (1961) 671–675.
[49] R.W. Heckel, An analysis of powder compaction phenomena, Trans. Met. Soc., AIME 221 (1961) 1001–1008.
[50] K.G. Pitt, M.G. Heasley, Determination of the tensile strength of elongated tablets, Powder Technol. 238 (2013) 169–175, https://doi.org/10.1016/j.powtec.2011.12.060.
[51] B. Bekaert, B. Van Snick, K. Pandelaere, J. Dhondt, G. Di Pretoro, T. De Beer, C. Vervaet, V. Vanhoorne, In-depth analysis of the long-term Processability of materials during continuous feeding, Int. J. Pharm. 614 (2022), 121454, https://doi.org/10.1016/j.ijpharm.2022.121454.
[52] P.H.M. Janssen, S. Depaifve, A. Neveu, F. Francqui, B.H.J. Dickhoff, Impact of powder properties on the rheological behavior of excipients, Pharmaceutics 13 (2021), https://doi.org/10.3390/pharmaceutics13081198.
[53] G. Thoorens, F. Krier, B. Leclercq, B. Carlin, B. Evrard, Microcrystalline cellulose, a direct compression binder in a quality by design environment - a review, Int. J. Pharm. 473 (2014) 64–72, https://doi.org/10.1016/j.ijpharm.2014.06.055.
[54] M.T. DeCrosta, J.B. Schwartz, R.J. Wigent, K. Marshall, Thermodynamic analysis of compact formation; compaction, unloading, and ejection: II. Mechanical energy (work) and thermal energy (heat) determinations of compact unloading and ejection, Int. J. Pharm. 213 (2001) 45–62, https://doi.org/10.1016/S0378-5173(00)00645-1.
[55] R. Mendez, C. Velazquez, F.J. Muzzio, Effect of feed frame design and operating parameters on powder attrition, particle breakage, and powder properties, Powder Technol. 229 (2012) 253–260, https://doi.org/10.1016/j.powtec.2012.06.045.
[56] J.K. Prescott, R.A. Barnum, On powder Flowability, Pharm. Technol. 24 (2000), 60-84+236.